Root Cause Analysis of Overlay metrology excursions with Scatterometry overlay technology (SCOL)

Karsten Gutjahr, Dongsuk Park, Yue Zhou, Winston Cho, Ki Cheol Ahn, Patrick Snow, Richard McGowan
GLOBALFOUNDRIES 400 Stone Break Extension, Malta, NY 12020

Tal Marciano*, Vidya Ramanathan*, Pedro Herrera, Tal Itzkovich, Janay Camp and Michael Adel
KLA-Tencor Corporation1 Technology Drive, Milpitas, CA 95035

ABSTRACT

We demonstrate a novel method to establish a root cause for an overlay excursion using optical Scatterometry metrology. Scatterometry overlay metrology consists of four cells (two per directions) of grating on grating structures that are illuminated with a laser and diffracted orders measured in the pupil plane within a certain range of aperture. State of art algorithms permit, with symmetric considerations over the targets, to extract the overlay between the two gratings. We exploit the optical properties of the target to extract further information from the measured pupil images, particularly information that maybe related to any change in the process that may lead to an overlay excursion. Root Cause Analysis or RCA is being developed to identify different kinds of process variations (either within the wafer, or between different wafers) that may indicate overlay excursions. In this manuscript, we demonstrate a collaboration between Globalfoundries and KLA-Tencor to identify a symmetric process variation using scatterometry overlay metrology and RCA technique.

Keywords: SCOL, Diffraction based overlay, Root Cause Analysis, overlay, target design, accuracy, litho metrology

I. INTRODUCTION

First order scatterometry overlay metrology on the A500 LCM relies on detection of the angular distribution of diffracted light from a pair of grating over grating structures for each direction of measurement. Such structures may be regarded as a grating resonator for which specific cavity modes travelling between the upper and lower gratings systematically appear in the wavelength spectrum. These modes manifest themselves as rapid variations in the intensity of the various diffracted spectral orders in certain narrow frequency bands [1]. The modes affect the accuracy of the overlay measurements and, in addition, are extremely sensitive to the grating over grating geometry. Any small changes in their structure, asymmetric or otherwise affect the modes in different ways. The advantage of measuring the signal in the pupil plane is to separate between different optical paths so that we can track with a single measurement setup any small changes in the grating over grating structure. We propose using such properties for identifying, classifying

*Tal.Marciano@kla-tencor.com
*Vidya.Ramanathan@kla-tencor.com

Metrology, Inspection, and Process Control for Microlithography XXX, edited by Martha I. Sanchez, Vladimir A. Ukrainstev
Proc. of SPIE Vol. 9778, 97781M · © 2016 SPIE · CCC code: 0277-786X/16/$18 · doi: 10.1117/12.2219668

Downloaded From: http://proceedings.spiedigitallibrary.org/ on 03/29/2016 Terms of Use: http://spiedigitallibrary.org/ss/TermsOfUse.aspx

and mapping process variations (PV) in order to monitor overlay metrology excursions. We will show that in addition to the classical overlay metrics, we can develop new metrics that can be used for creating wafer maps of process variations without any additional measurement requirements. In parallel, this methodology also lets us identify the most robust on-tool measurement setup.

In the next section we start by providing a brief review of scatterometry overlay using the A500 LCM tool, followed by an introduction to landscapes and root cause analysis in section 3. In section 4 we outline the details of the design on experiments followed by the RCA simulations in section 5. Finally we present the results in section 5 and conclude in the section thereafter.

II. SCATTEROMETRY OVERLAY

Measuring scatterometry overlay or SCOL technology on an A500 LCM tool consists of recording the first diffracted orders from a 4-cell SCOL target (2-cells per axis) in the pupil or the Fourier plane.

In the SCOL algorithm D_i , the per pixel differential signal between the two diffracted orders for each cell, is modelled in the following way:

$$D_{1,2} = A sin \frac{2\pi}{P} (OVL \pm f_0) \qquad (1)$$

Where A is the amplitude, OVL is the overlay, P, the periodicity (pitch) of the two gratings, and f_0 the induced offset between the two cells of the target. Importantly, while the overlay OVL, is the same for all pupil pixels, the amplitude A is not.

We attempt to identify two kinds of process variations, either within a wafer or among different wafers – (a) Symmetric PV: changes to the diffracted pupil signal due to optical path length changes stemming from changes in thickness or dispersion, coming from one of the under layers. (b) Asymmetric PV: changes to the diffracted pupil signal due to target asymmetry such as SWA changes or pad-to-pad variations, etc.

Before proceeding to more details, it is useful to define the following two metrics [2]:
$SyS(px, \lambda) = (D_1 - D_2)/2f_0$, which is an estimate for the overlay sensitivity of a given target. It is to be noted that the *SyS* metric is insensitive to any asymmetric process variations over the targets and $ASyS(px, \lambda) = (D_1 + D_2)/2f_0$, a metric to detect breaking of symmetry in the pupil signal that maybe or may not be induced by overlay. Ideally, if the target has no imperfections, the *ASyS* metric is sensitive to breaking of symmetry due to overlay, but in the presence of process variations like grating asymmetry, the *ASyS* would also sense additional breaking of symmetry which would lead to inaccuracy in the overlay measurements.

The overlay per pixel is defined to be –

$$OVL(p, \lambda) = f_0 ASyS/SyS \qquad (2)$$

For a wafer with no imperfections or an ideal signal, $ASyS(px, \lambda) = \epsilon SyS(px, \lambda)$ and overlay and defined as - $OVL(px, \lambda) = OVL$ ($\epsilon = OVL/f_0$). In the presence of process variations, when *SyS* approaches zero, then the difference between the per pixel overlay and the true overlay is dramatically increased – this phenomenon is indicative of a resonance [3]. The advantage of measuring the pupil information lies in the fact that every pixel in the pupil corresponds to a different optical path. The resonance condition manifests itself as an 'arc' in the pupil image (fig.

Downloaded From: http://proceedings.spiedigitallibrary.org/ on 03/29/2016 Terms of Use: http://spiedigitallibrary.org/ss/TermsOfUse.aspx

1). The 'arc' corresponds to a collection of pixels wherein the optical path length satisfies the resonance condition.

In the technique to calculate overlay using angle resolved pupil information, the SCOL algorithm can screen certain pixels whose *SyS* values are too close to zero; this considerably attenuates the resonance effect over the accuracy of the measurements. Also, if the process is perfectly controlled, measuring in resonance will not affect accuracy of measurement in the pupil plane.

III. LANDSCAPES AND ROOT CAUSE ANALYSIS

The RCA methodology tracks the appearance of the resonance over the pupil in different targets on a wafer as well as various overlay metrics to identify and quantify different kinds of process variations.

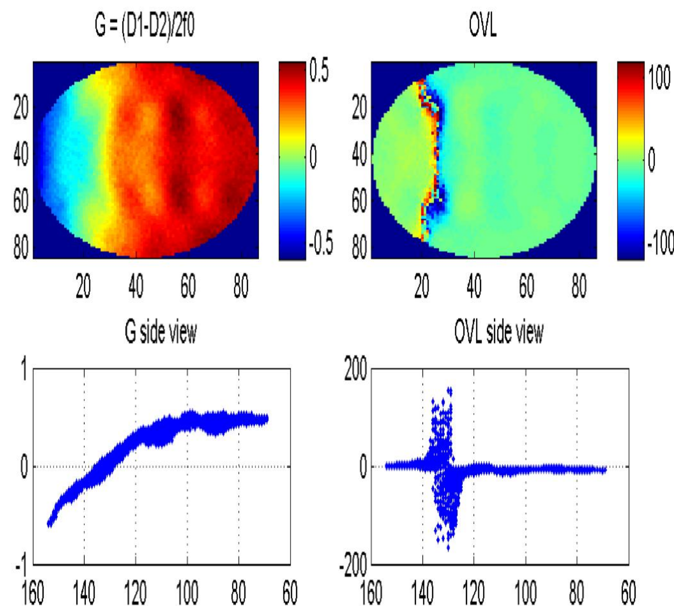

Fig. 1. Calculated *SyS* value for each pixel in the pupil image (top left), corresponding overlay values (top right) and their respective cross sections (bottom left and right). The corresponding recipe or measurement setup is to be in resonance as *SyS(p)* crosses zero giving rise to an 'arc' of resonance in the per-pixel overlay.

Sensitivity of resonance to Process Variations

For a given grating-on-grating target, the film stack underneath the target possesses a specific number of resonances over the measurement spectrum and the pupil average overlay metrics can be described by a specific landscape (LS) [3]. In fig. 2. we demonstrate a simulated landscape shift on a hypothetical stack. We vary the height of the fins in the under layer and simulate the corresponding movement in the landscape.

When in resonance, the discontinuity in the pupil indicates an increased overlay inaccuracy and $Pupil3\sigma$ (fig. 3). In case of symmetric process variations over the wafer such as thickness variation

Downloaded From: http://proceedings.spiedigitallibrary.org/ on 03/29/2016 Terms of Use: http://spiedigitallibrary.org/ss/TermsOfUse.aspx

of one or more of the under layers and CD variations, or variation that do not break target symmetry, the LS and thus the ‘arc’ in the pupil are shifted. An illustration of this phenomenon can be done with guided modes in a cavity. The thickness of the cavity or its optical properties will influence the appearance and the number of the resonant modes within the cavity.

Since asymmetric PV are not influenced by SyS values, no shift in the landscape is observed but the $Pupil3\sigma$ and the overlay inaccuracy will scale in consequence (schematic representation in fig. 4). When the asymmetry is increased (with no change in the symmetric PV), the arc would appear at the same region over the resonant pupil but with an increased $Pupil3\sigma$.

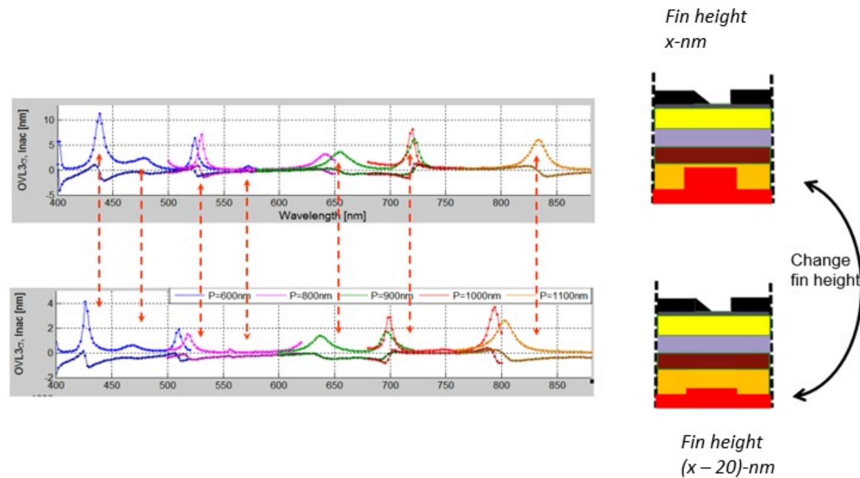

Fig. 2. Landscape shifts in case of symmetric process changes for a hypothetical stack. The LS of pupil 3S and overlay is represented as a function of targets with different pitches. The different colors over the spectrum indicate the different pitches in the simulated targets as indicated in the legend.

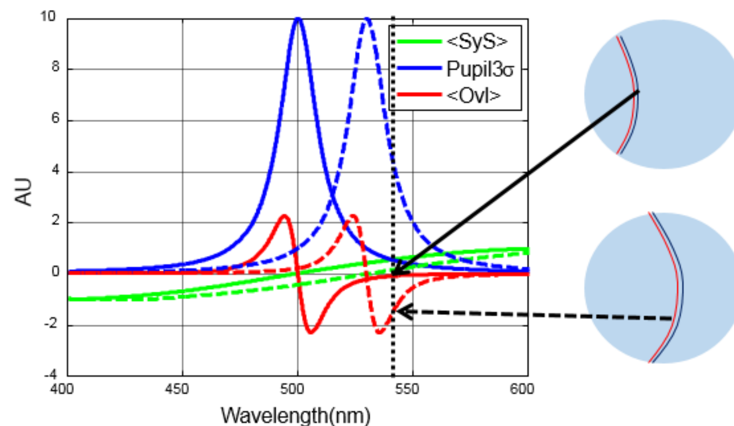

Fig. 3. Schematic illustration of the landscapes of the $Pupil3\sigma$ and the overlay as a function of wavelength. In case of symmetric process variations, the peak of resonance is shifted (shifts to the red end of the spectrum with increasing thickness and blue shifted as thickness decreases). A schematic diagram of the corresponding ‘arc’ movement within the pupil is represented as well.

Downloaded From: http://proceedings.spiedigitallibrary.org/ on 03/29/2016 Terms of Use: http://spiedigitallibrary.org/ss/TermsOfUse.aspx

IV. DESIGN OF EXPERIMENT

In order to experimentally validate the root cause analysis, we designed a set of four DOE wafers for the STI layer on a 14-nm product. Each of the 4 wafers were prepared with a different trench height (fig. 5) induced with a timed-etch process. The induced height differences scaled from -20nm to +60nm from the height of record or the POR trench height. This varying height between the different wafers mimics a symmetric process variation

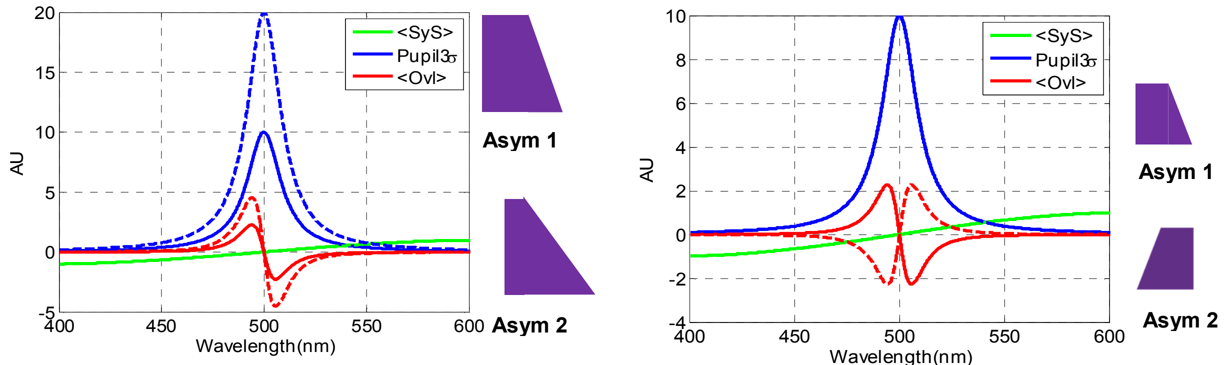

Fig. 4. Schematic illustration of the landscapes of the $Pupil3\sigma$ and measured overlay in case of an asymmetric process variation. Left - asymmetry is increased (bold lines v.s dotted line). Right - the magnitude of the asymmetry remains the same but measured overlay changes signs (i.e: left SWA VS. right SWA asymmetry).

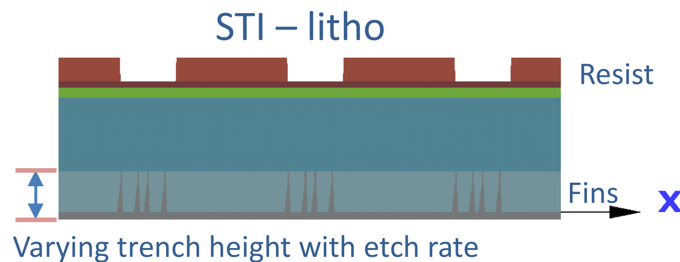

Fig. 5. Schematic drawing of the stack and the DOE conditions for the experimental verification.

Diffraction based overlay data from a particular target was collected from an A500 LCM tool for each wafer for every laser wavelength, polarization and apertures available on the tool. The RCA calculations were performed offline using the raw pupil signals from the measurements.

V. RCA SIMULATIONS

Using the pupil information recorded on the POR wafer, we defined various metrics that would let us identify an on-tool measurement condition that was robust or insensitive to the induced process variation and a different measurement condition that was sensitive to pick up the induced variations. We define the following metrics that were used in our offline calculations –

Downloaded From: http://proceedings.spiedigitallibrary.org/ on 03/29/2016 Terms of Use: http://spiedigitallibrary.org/ss/TermsOfUse.aspx

1. ***SyS*, Symmetric Signal:** Metric that is insensitive to symmetry breaking and enables tracking of symmetric process variations within wafer and between wafers.
2. **Pupil Flatness:** Metric defined between 0 and 1 wherein 0 corresponds to a perfectly flat pupil indicating high process robustness and 1 corresponding to an unstable region that is highly sensitive to process variations.
3. **Pupil 3S ($Pupil3\sigma$):** Variance of the calculated overlay over the pupil signal
4. **Arc Index:** Binary metric; 1 or 0 indicating presence or absence of resonance in the pupil respectively.
5. **Sensitivity:** Target sensitivity to measure overlay

We evaluated the performance of various different recipe setups classified as per our newly defined metrics. By comparing the $Pupil3\sigma$, pupil flatness and sensitivity metrics for both X and Y cells we observe that one of the red wavelengths and *'P'* polarizations on the tool (we will indicate this setting as *Red1P*) is most resistant to process changes, making it a robust setup to measure overlay whereas the *Red2P* setup is the least resistant to process changes. Recipe robustness is demonstrated by the lack of 'arcs' in the pupil overlay combined with none of the pixels within the *SyS* metric, with the numerical value of zero (figure 6).

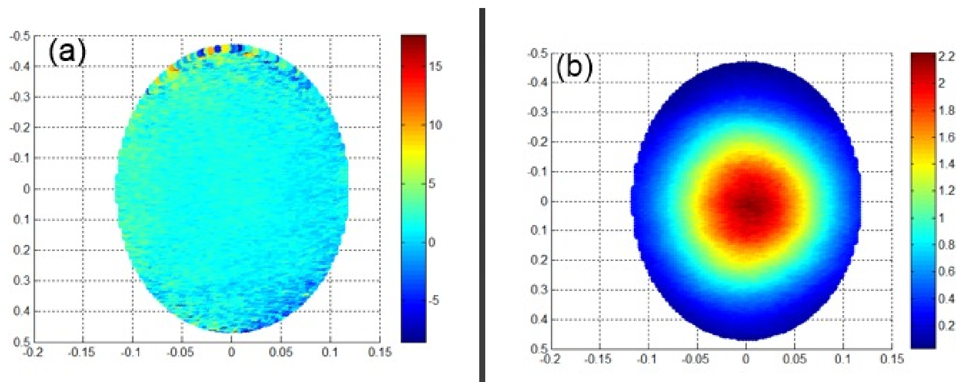

Fig. 6(a) – $Pupil3\sigma$ and (b) *SyS* metric for the robust recipe setting of *Red1P* on the tool. Note that the pupil overlay has no 'arcs' in it and the *SyS* metric has no zero crossings either.

On the other hand, the process sensitive setting (which we denote here as *Red2P*) has the 'arcs' in the $Pupil3\sigma$ with the corresponding zero value pixels in the *SyS* metric as in figure 7.

VI. RESULTS

Root cause analysis calculations were performed on all the DOE wafers. By comparing the pupil analytics and the *SyS* metric for all the wafers, we were able to rank the 4 wafers in an ascending order of the trench height (Fig.8). We observe that the 'arc' in the $Pupil3\sigma$ starts in the center and travels towards the edge of the pupil as the trench height increases. This phenomenon is consistent with an increase in the optical path length that is caused by the different trench heights induced by the etch process. We confirmed the experimental results by a pilot simulation run. We simulated the stack underneath the gratings for each DOE wafer. Simulations were run considering

Downloaded From: http://proceedings.spiedigitallibrary.org/ on 03/29/2016 Terms of Use: http://spiedigitallibrary.org/ss/TermsOfUse.aspx

the incident angles and wavelength used in the most sensitive measurement setup (*Red2P*). By comparing the simulated $Pupil3\sigma$ for each case, we observed that the 'arc' in the pupil signal moves to the edge of the pupil with increasing trench height (fig.9) just as it does in our experimental results.

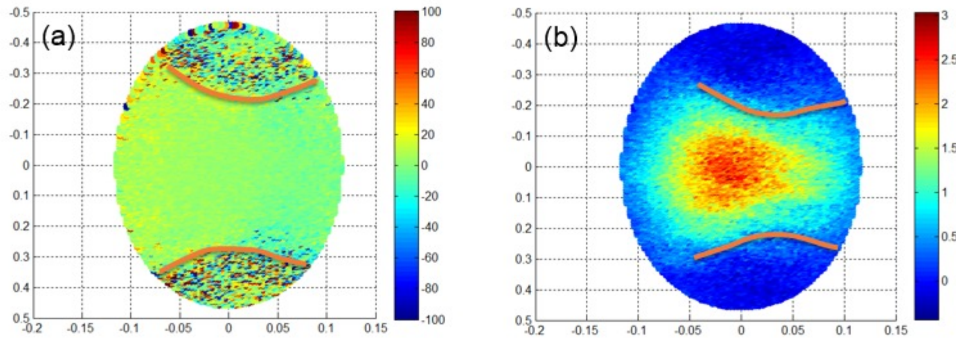

Fig. 7 (a) – $Pupil3\sigma$ and (b) *SyS* metric for the process sensitive recipe setting of *Red2P* on the tool. There are 2 arcs in the pupil overlay and corresponding 2 regions of zero crossing in the *SyS* metric signal. (The orange arcs are drawn to serve as a guide to the eye).

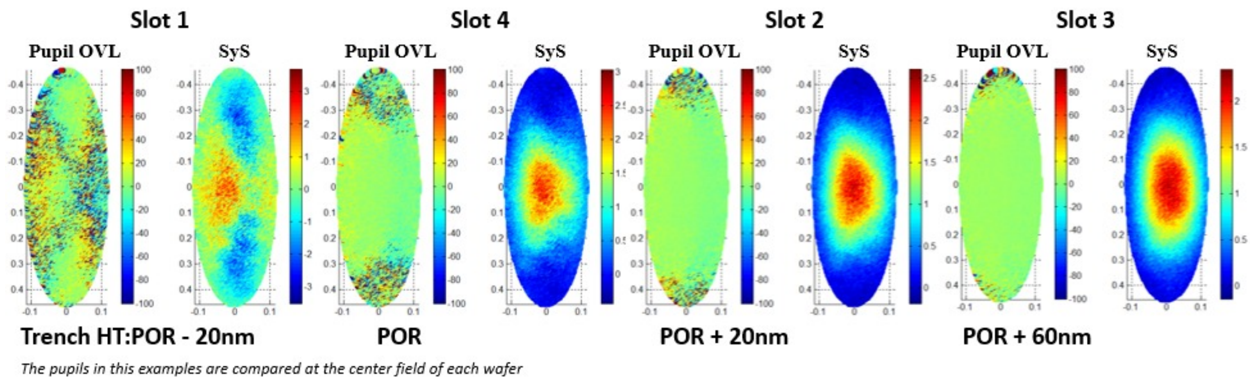

Fig. 8. $Pupil3\sigma$ and *SyS* metric for each DOE wafer ranked in ascending order for trench height.

The symmetric process variation is also captured when plotting the wafer averaged *SyS* metric for each wafer as a function of increasing trench height (fig. 10). We can use the metrics to construct a process window for the trench height parameter. When plotting the various metrics such as the pupil flatness and the $Pupil3\sigma$ for the different DOE wafers, we observe that the robust recipe setting of *Red1P* enters into the sensitive zone as the trench height increases over +20nm from the POR height (fig.11). One can also compare the merit of other recipe settings and choose an overlay measurement setting on the tool with a wide process window for a given parameter.

Also these metrics can be monitored as part of fab-wide statistical process control that would let the metrology engineer keep track of any process changes that may occur.

Downloaded From: http://proceedings.spiedigitallibrary.org/ on 03/29/2016 Terms of Use: http://spiedigitallibrary.org/ss/TermsOfUse.aspx

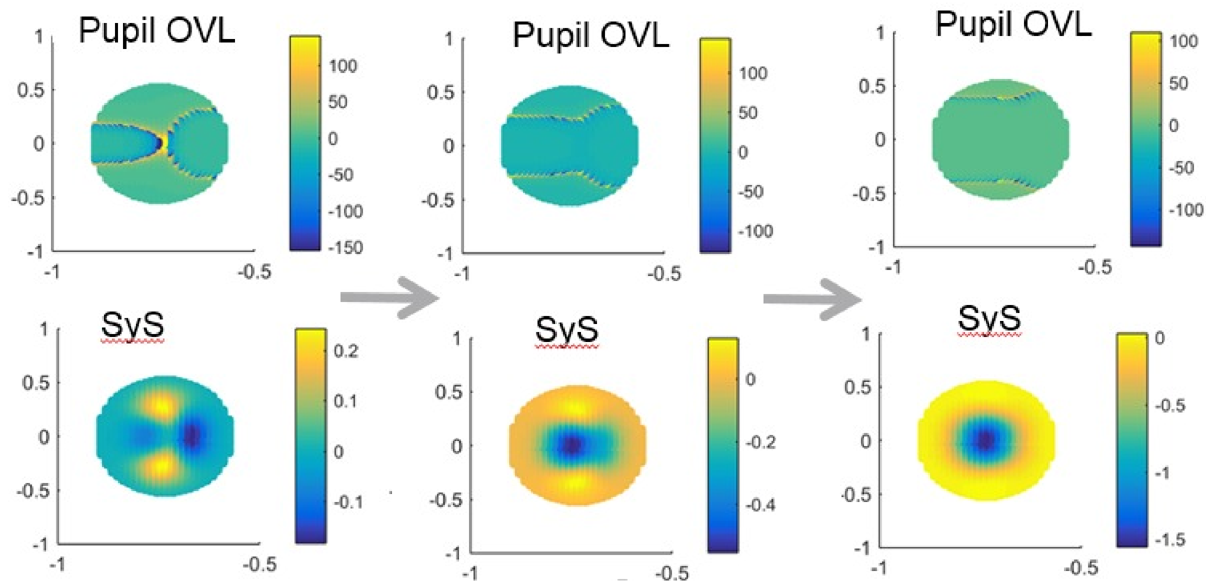

Fig. 9. Simulated pupil OVL and *SyS* metric for various trench height. Simulations agree with experimental data indicating that RCA analysis is able to identify the underlying symmetric process variations.

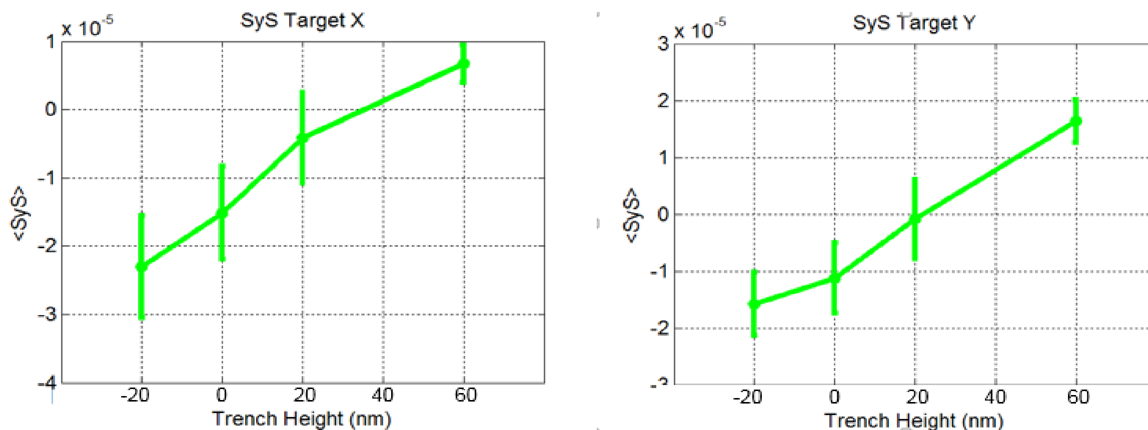

Fig. 10. The SyS metric is monotonically increasing with the trench height due to varying etch time between wafers indicating that the symmetric process variation due to etch is clearly identified.

We have tried to estimate the trench height variation across each individual wafer for the 4 DOE wafers. We start by assuming a linear relationship between the *SyS* metric and the trench height (fig.10). By fitting a linear curve through the plots in fig. 10, we convert the slope of the SyS metric to a length scale. This lets us plot a wafer map (fig. 12) for the all 4 cases indicating the difference in trench height from the height of record or POR height. This lets us observe the variation of the parameter over each wafer.

Downloaded From: http://proceedings.spiedigitallibrary.org/ on 03/29/2016 Terms of Use: http://spiedigitallibrary.org/ss/TermsOfUse.aspx

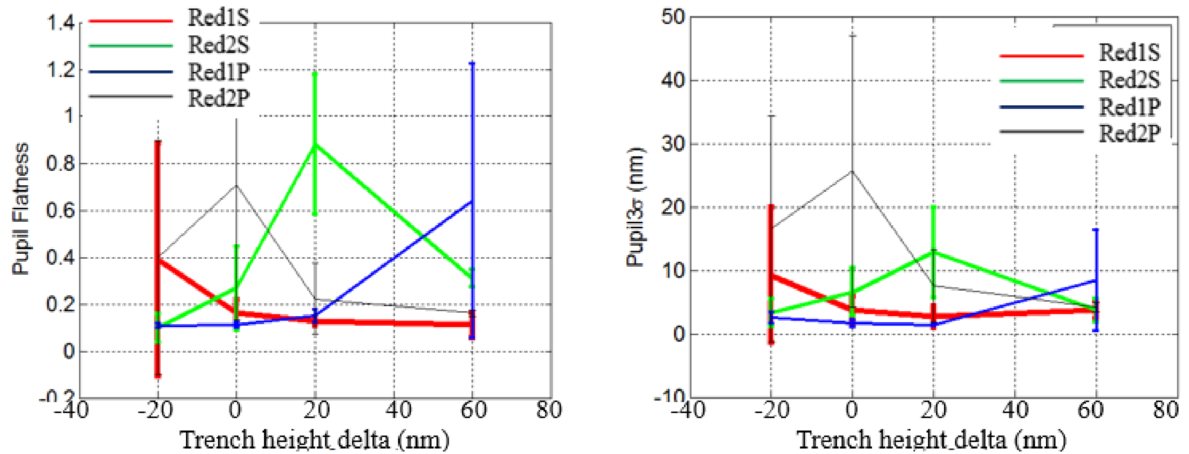

Fig. 11. *Red1P* recipe setting previously identified as process robust recipe remains robust for a trench height of POR - 20nm, POR and POR + 40nm, but reaches 10nm for POR + 60nm. RCA analysis identifies the root cause of the process excursion as a symmetric process variation due to etch.

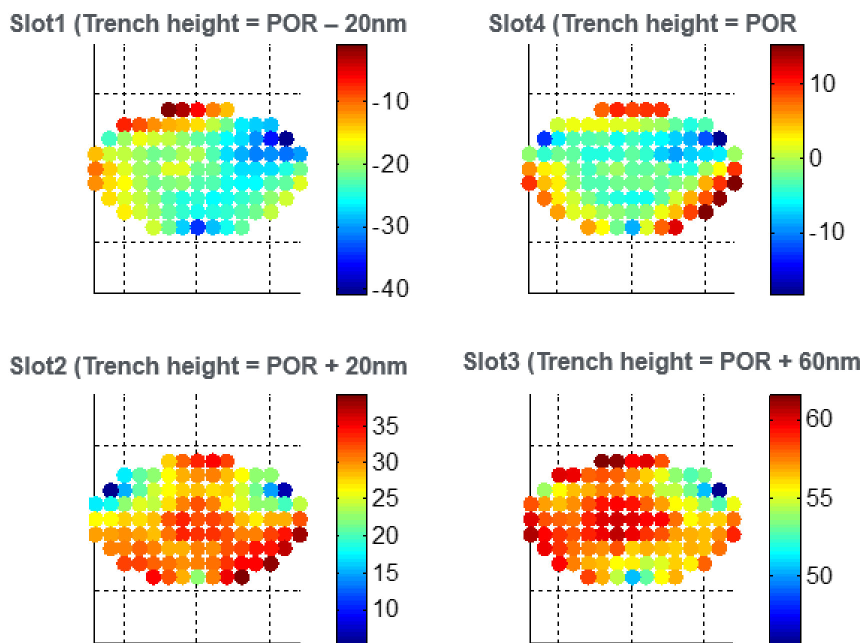

Fig. 12. Trench height variation across the wafer; estimated using the slope from the plots of the *SyS* metric to the trench height difference (fig.10).

VII. CONCLUSION

For the overlay target investigated, we observe that the automatic recipe optimization algorithm (ARO) on A500 LCM tool can identify a process robust recipe and offline root cause analysis (RCA) can identify a process sensitive recipe in the event of large process variations.

Downloaded From: http://proceedings.spiedigitallibrary.org/ on 03/29/2016 Terms of Use: http://spiedigitallibrary.org/ss/TermsOfUse.aspx

Offline root cause analysis (RCA) can classify a process excursion as due to either asymmetric or symmetric process variation.

We believe that the RCA tool can be extremely beneficial to metrology engineers to not only identify process excursions but to also be able to classify the excursion in terms of symmetric or asymmetric variations.

Acknowledgments

The authors would like to acknowledge Ankit Jain of KLA-Tencor for all the discussions that lead to the final stack configuration used in the simulations.

References

1. A Hessel and A. A. Oliner, 'A new theory of Wood's anomalies on Optical gratings', Applied optics, Vol. 4 pg. 1275, 1965.

2. Mike Adel, Daniel Kandel, Vladimir Levinski, Joel Seligson, Alex Kuniavsky, 'Diffraction order control in overlay metrology: a review of the roadmap options' Proc. SPIE 6922, Metrology, Inspection, and Process Control for Microlithography XXII, 692202 (March 14, 2008); doi:10.1117/12.773243.

3. Daniel Kandel, Mike Adel, Berta Dinu, Boris Golovanevsky, Pavel Izikson, Vladimir Levinski, Irina Vakshtein, Philippe Leray, Mauro Vasconi, Bartlomiej Salski, 'Differential signal scatterometry overlay metrology: an accuracy investigation' Proc. SPIE 6616, Optical Measurement Systems for Industrial Inspection V, 66160H (June 18, 2007).

4. Daniel Kandel, Vladimir Levinski, Noam Sapiens, Guy Cohen, Eran Amit, Dana Klein, Irina Vakshtein, 'Overlay accuracy fundamentals' Proc. SPIE 8324, Metrology, Inspection, and Process Control for Microlithography XXVI, 832417 (March 29, 2012).

5. Guy Cohen, Eran Amit, Dana Klein, Daniel Kandel, Vladimir B. Levinski, 'Overlay quality metric' Proc. SPIE 8324, Metrology, Inspection, and Process Control for Microlithography XXVI, 832424 (March 29, 2012); doi:10.1117/12.916379.

Downloaded From: http://proceedings.spiedigitallibrary.org/ on 03/29/2016 Terms of Use: http://spiedigitallibrary.org/ss/TermsOfUse.aspx